Alexandria Engineering Journal (2011) **50**, 91–104

Alexandria University

Alexandria Engineering Journal

www.elsevier.com/locate/aej
www.sciencedirect.com

ORIGINAL ARTICLE

Finite element analysis of beam-to-column joints in steel frames under cyclic loading

Elsayed Mashaly, Mohamed El-Heweity *, Hamdy Abou-Elfath, Mohamed Osman

Structural Engineering Department, Faculty of Engineering, Alexandria University, Alexandria, Egypt

Received 19 June 2010; accepted 21 November 2010
Available online 5 May 2011

KEYWORDS

Finite element method;
Moment resisting steel frames;
Cyclic loading;
Beam-to-column connections;
Extended end plate connection

Abstract The aim of this paper is to present a simple and accurate three-dimensional (3D) finite element model (FE) capable of predicting the actual behavior of beam-to-column joints in steel frames subjected to lateral loads. The software package ANSYS is used to model the joint. The bolted extended-end-plate connection was chosen as an important type of beam–column joints. The extended-end-plate connection is chosen for its complexity in the analysis and behavior due to the number of connection components and their inheritable non-linear behavior. Two experimental tests in the literature were chosen to verify the finite element model. The results of both the experimental and the proposed finite element were compared. One of these tests was monotonically loaded, whereas the second was cyclically loaded. The finite element model is improved to enhance the defects of the finite element model used. These defects are; the long time need for the analysis and the inability of the contact element type to follow the behavior of moment–rotation curve under cyclic loading. As a contact element, the surface-to-surface element is used instead of node-to-node element to enhance the model. The FE results show good correlation with the experimental one. An attempt to improve a new technique for modeling bolts is conducted. The results show that this technique is supposed to avoid the defects above, give much less elements number and less solution time than the other modeling techniques.

1. Introduction

The behavior of beam-to-column joints in steel frames can be conveniently represented by its flexural behavior which is primarily shown by the moment–rotation (M–θ) relationship. This behavior is non-linear even at low load levels. In fact, moment–rotation curves represent the result of a very complex interaction among the elementary parts constituting the connection.

The potential economic implication of connections on frame design is realized by code provisions [1,2]. As a result,

* Corresponding author.

Peer review under responsibility of Faculty of Engineering, Alexandria University.
doi:10.1016/j.aej.2011.01.012

Production and hosting by Elsevier

special design guides for moment resisting connections have been developed [3,4]. Since the connection types are highly indeterminate, current design approaches cannot model three-dimensional (3D) systems which are governed by complex combined material and geometrical non-linearities, friction, slippage, contact, bolt–end plate interactions and, eventually, fractures. Hence, the finite element technique has been adopted as a rational supplement to the calibration of design models.

Krishnamurthy was the pioneer in the field of 3D modeling of connections, by adopting eight-node sub-parametric bricks in order to reproduce the behavior of bolted end plate connections [5]. The analyses carried out were linearly elastic but expensive, because contact was embodied artificially by attaching and releasing nodes at each loading step on the basis of the stress distribution. Bolt preloading phenomena were simulated also. Then, a correlation between two-dimensional (2D) and 3D finite element analyzes was established and a parametric study was conducted with 2D models, owing to the limited computer capabilities. A similar procedure was proposed by Kukreti et al. [6] in order to reproduce moment–rotation relationships of end plate connections. The results of these analyses were useful in the range for which such validations were performed. However, fundamental issues relating to the number of integration points, kinematic description, element type and discretization were not investigated. Kukreti et al. [7] also developed finite element models for stiffened steel tee-hanger connections. These models can be classified as hybrid since they encompassed solid elements for both plates and bolts and plane elements for both web and stiffeners. Satisfactory results were obtained using these models. Nevertheless, some basic issues like discretization and type of yield criterion were faced up.

Researchers used 3D finite element models based either on shell and separator truss elements [8] or shell and contact elements [9], in order to simulate end plate as well as beam and column flange behavior. The agreement between simulations and test data was satisfactory because both contact and beam elements were adopted to simulate friction and bolt action, respectively. But, so far as the simulation of prying forces is concerned, thick shell analysis is capable to simulate the evolution of internal normal stresses required to satisfy equilibrium with prying forces.

A rigorous approach to the modeling of bolted connections was adopted later by Gebbeken et al. [10], which discretized bolted tee stubs in a 3D fashion by means of eight-node brick elements, and investigated the contact problem between deformable bodies in a small deformation regime. Comparisons between simulated and measured data were good. However, the parametric study on end plate joints was performed with 2D finite element models, thus limiting the analysis effectiveness. 3D finite element models based on solid and contact elements of the ABAQUS library [11,12] were proposed by Bursi and Leonelli [13] to simulate the rotational behavior of isolated bolted end plate connections.

In this study, a three-dimensional model using the finite element analysis with material non-linearities is introduced. The main purpose of the proposed finite element (FE) model is to simulate the moment–rotation behavior of extended end-plate connections subjected to either monotonic or cyclic loads. This model has the ability to be modified easily and then resolved repeatedly to take the different geometric and material parameters that affect the behavior of such joints into account.

2. Beam-to-column joint under monotonic load

In order to analyze beam-to-column joint under lateral monotonic load, a finite element model is presented using the software package ANSYS [14]. The model is utilized to investigate the results of both experimental and theoretical models made by Khalil [15] for steel beam-to-column connections.

2.1. Joint configuration

Fig. 1 shows the typical configuration of the joint which consisted of a rectangular end-plate welded to the beam

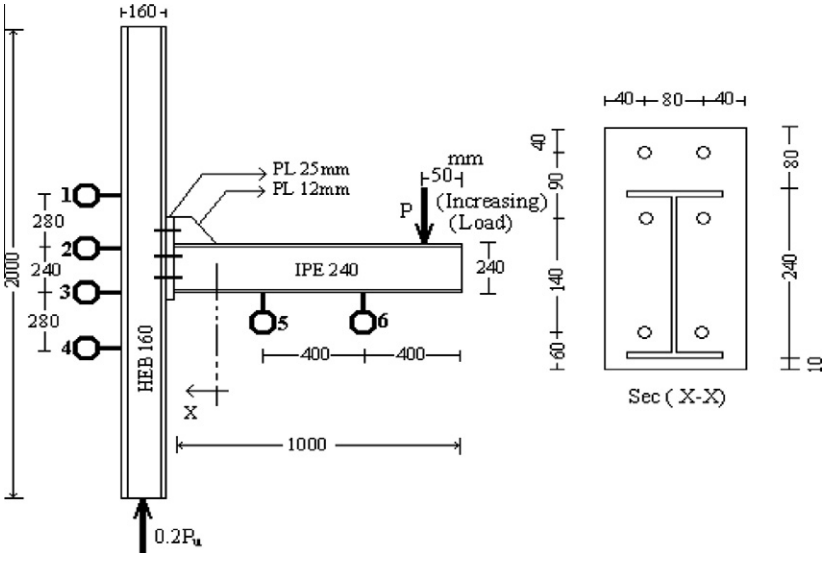

Figure 1 Beam-to-column steel joint by Khalil [15].

cross-section and fixed to the column flange by three rows of bolts of diameter 22 mm, M22, and grade 10.9, two of them at the tension side of the connection (one above and the other below the tension beam flange) and the third above the compression beam flange. The dimensions of the used bolts and its nuts are shown in Fig. 2.

2.2. Loading system

For the studied joint, two concentrated loads were used. The first acted axially on the bottom of the column (upward) to generate constant concentrated load equal to $0.2P_u$ [15]. The second load increasingly acts 50 mm away from the tip of the beam to generate an increasing bending moment during the loading, as shown in Fig. 1. Six dial gauges were used to measure both the vertical and horizontal displacements of the connection. Dial gauges from 1 to 4 were used for horizontal displacements, whereas gauges 5 and 6 were used for vertical displacements.

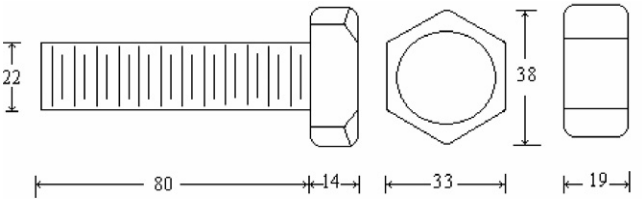

Figure 2 Dimensions of bolts and nuts (M22 Grade 10.9) in mm.

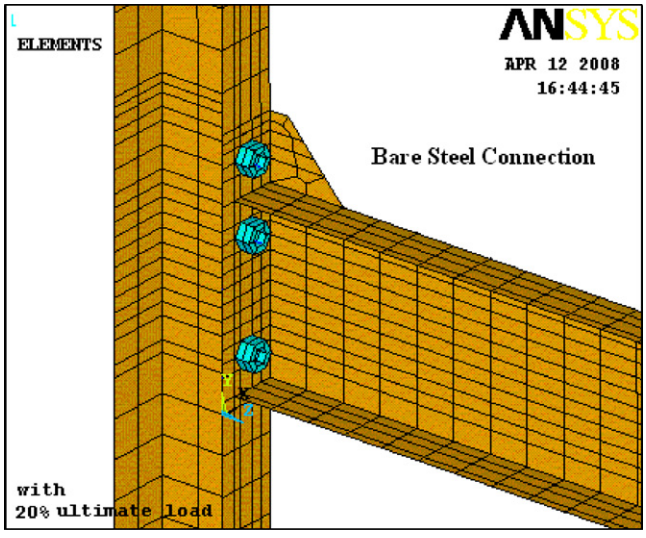

Figure 3 General view of the studied connection under monotonic loading.

2.3. Finite element model

The details of the finite element model used in this part are very closely based on the models presented by Sherbourne and Bahaari [9], Khalil [15], and Bahaari and Sherbourne [16] (Fig. 3). Node-to-node contact elements and hybrid bolts are used in the modeling. Due to symmetry about a plane passing through the beam and column webs, only one half of the connection is considered in the modeling.

2.3.1. Element types

Different finite element types in the ANSYS software package are used in the modeling of beams, columns, end-plates, and bolts. These elements are: **SHELL43** (4-Node Plastic Large Strain Shell) was used to model beam, column, end-plate and stiffeners. **SOLID45** (8-Node 3D Structural Solid) was used to model bolt head and nut. Since head and nut stay in contact with their connecting plates through all load steps, they are defined as continuous with both column flange and end-plate nodes, respectively. **LINK8** (3D Spar or Truss Element): The bolt shank is modeled using six 3D spar elements connecting the farthest corner nodes of head and nut to each other. Though these elements overlap the plate holes elements, there is no mathematical connection between them. Using six spar elements to model the bolt shank allows finding the magnitude, distribution, and the direction of the bolt force within the section. This is especially important for thin end-plates in which the bolts in tension undergo considerable biaxial bending. The spar elements carry only axial forces and any shear on the interface between end-plate and the column flange will be transferred through the friction allowed by the contact elements. **CONTAC52** (3D Point–Point Contact Element): One of the interesting and at the same time difficult aspect of bolted connection analysis is the unpredictability of the actual support conditions at the back of the end-plate. Obviously, the plate would pull away from the adjacent column flange around the beam tension flange to a varying extent depending upon the beam and end-plate dimensions, bolt size and position, material properties and, especially, the load level. At the same time, when the end-plate tends to bear against the

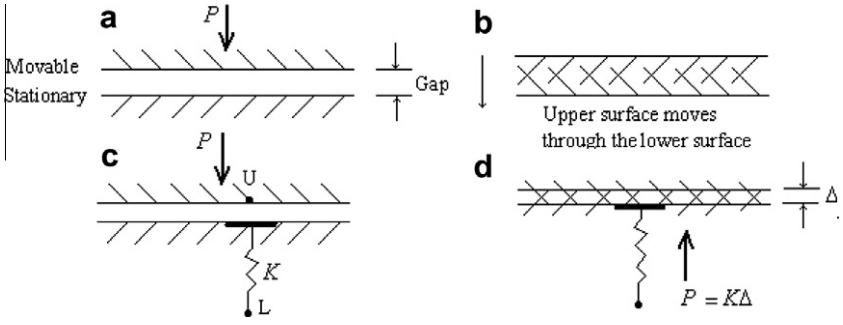

Figure 4 Interface element mechanism.

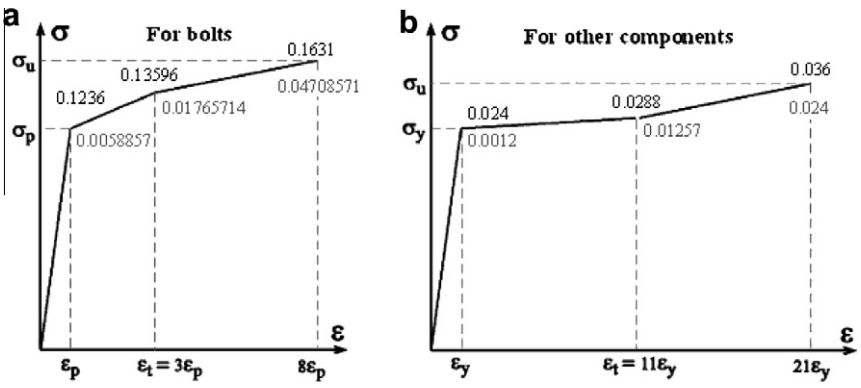

Figure 5 Tri-linear stress–strain curve: (a) for high strength bolts; (b) for steel sections.

column flange, it should not move freely through the adjacent component.

Therefore, the boundary at the back of the end-plate is a variable boundary-value problem that can be solved only by an interactive approach. Fig. 4 explains the mechanism of the interface (contact) between two surfaces when modeled using finite element. In the beginning, the two surfaces are far from each other since no stiffness exists between the surfaces (Fig. 4a). If the upper surface displaces downward due to a force P, it will move through the lower surface as it does not exist (Fig. 4b). Attaching a spring of stiffness (K) to the nodes of the lower surface will only carry load when the gap closes in compression (Fig. 4c). Therefore, when the upper surface contacts the lower one, a spring force develops to prevent the upper surface from moving through the lower one. Equilibrium will be achieved when $K\Delta = P$ (Fig. 4d). The amount of "pass through" Δ will therefore depend on the spring stiffness K. Real surfaces have zero material overlap meaning that interface stiffness $K = \infty$. However, using a very high stiffness causes numerical problems in the equation solver and convergence difficulties in problems with multiple inter-surface elements. Practically, the required value of K is the one which allows an accepted very small amount of overlap between the two surfaces.

According to the ANSYS software package, it is recommended that the interface stiffness K is taken between 17.5

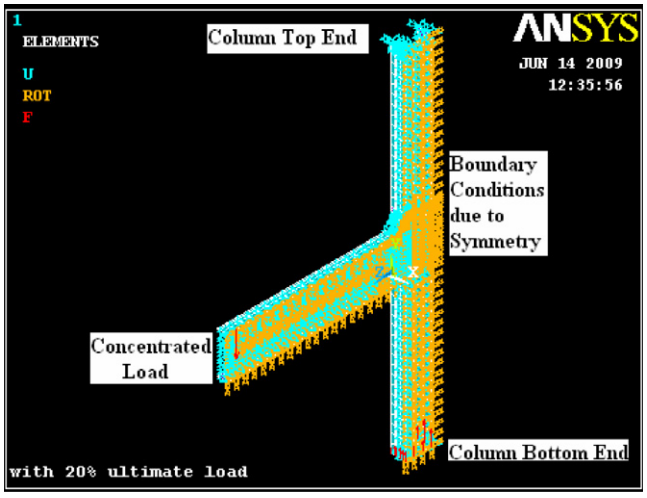

Figure 6 Boundary conditions [load and constraints].

Table 1 Axial forces in the bolts.

Location of bolt	Axial force (ANSYS) (ton)	Axial force in Ref. [15] (ton)	Percentage of difference (%)
Upper bolt	6.02	6.49	7.2
Intermediate bolt	3.32	3.44	3.49
Lower bolt	0.487	0.32	52

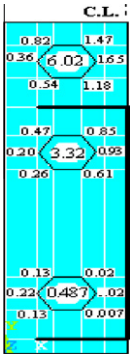

Figure 7 Forces in the links of the bolts shanks.

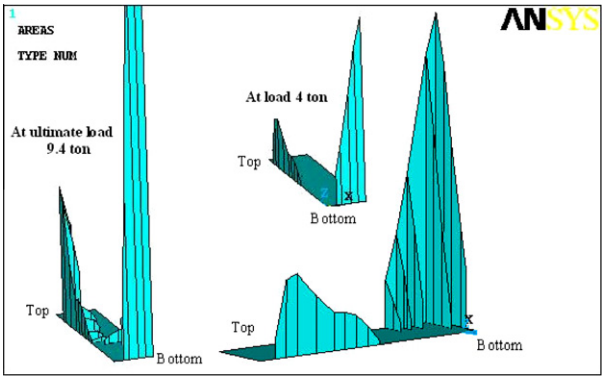

Figure 8 Contact force distribution.

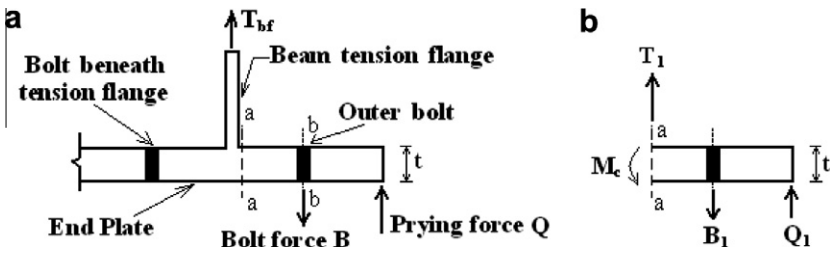

Figure 9 Prying forces.

and 1750 ton/mm. Bahaari and Sherbourne [16] suggested that $K \approx 5EA/nt$ where E is the modulus of elasticity, A the end-plate area, t the minimum of the thicknesses of end-plate and column flange, and n is the number of interface elements connecting the two surfaces. Within these limits, CONTAC52 was used to model the contact between the end-plate and the adjacent column flange with coefficient of friction equals to 0.3 and interface stiffness of (17.5 ton/mm). Only the corner nodes of elements are connected. A coefficient of friction is defined for sliding resistance while the interface is closed. Thus, The CONTAC52 element (gap) will act only in compression producing axial compressive force in the element and it will transfer the shear through the friction. Whenever axial tension exists, the element will break and the sliding between the two surfaces will occur (no shear transfer).

2.3.2. Material properties

The stress–strain curves are taken as elastic-strain hardening. This is acceptable since strain hardening is paired with excessive yielding in large areas and a large deflection criterion governs the ultimate strength design. However, in end-plate connections excessive strain is mostly local and besides considerable shear stresses occur in the region between the top bolts and the beam tension flange which necessitates considering strain hardening. Stress–strain curves for HS (high strength) bolts, and steel sections, with the values of stresses and strains, are shown in Fig. 5a and b, respectively.

2.3.3. Yield criterion

The von Mises yield criterion is used to predict the onset of the yielding. The behavior upon further yielding is predicted by the "flow rule" and "hardening law". The associative flow-rule for the von Mises yield criterion, i.e., Prandtl–Reuss flow equations is used along with hardening of steel sections and bolts to model the Bauschinger effect. Kinematic hardening is assumed for modeling of the steel connection assuming that the yield surface only transfers in the direction of yielding and does not grow in size.

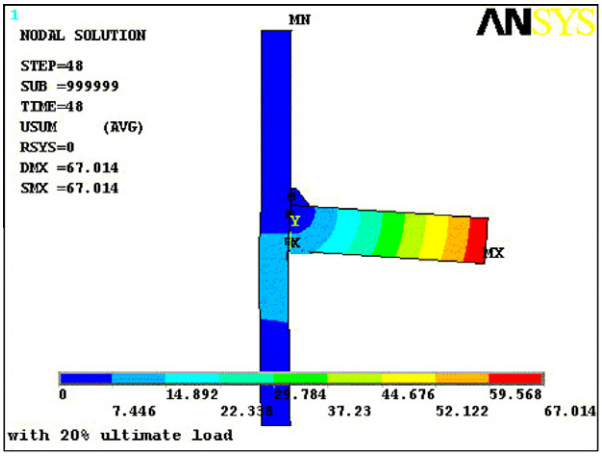

Figure 10 Deformed shape of the connection just before failure.

2.3.4. Boundary conditions

Upper column end is a pinned support while the lower end is a roller support along the vertical axis (direction of the column axis), as shown in Fig. 6. Due to symmetry, only half of each connection is modeled. Symmetric displacement boundary conditions are defined for the nodes along the plane of symmetry.

2.4. Results of the FE modeling

The main aim of this section is to declare the accuracy of the results obtained by the finite elements models established using ANSYS.

2.4.1. Connection bending moment

The connection bending moment is transferred by both axial tension in the bolts and compressive forces in the contact elements between the end-plate and the column flange.

2.4.1.1. Axial forces in bolts. Table 1 and Fig. 7 show the axial forces in the shanks of the bolts at load level 4.0 ton as an example. The difference in the lower bolt is large since the value itself is small. Also, Fig. 7 shows that the axial forces in the links of tension bolts near the axis of symmetry (beam web) are greater than those far away from the axis of symmetry.

2.4.1.2. Compression forces in contact elements. Fig. 8 shows the distribution of the contact forces between the end-plate and the column flange. There are two main regions, the first is on the bottom part (near to the beam compression flange) and the second is on the top part (near the most stressed bolts on the upper outer side) resulting from the prying forces on the connection.

2.4.2. Prying action

External tension in a bolted connection will reduce the contact pressure between end-plate and column flange. Also, the relative size of bolt and plate thickness causes changes of curvature along the free edges of the extended portion. However, depending on the relative flexural rigidities of the plate and the column flange, additional forces may be developed near the plate tip or edge called prying forces. These forces are

necessary to balance plate bending. Prying forces (especially their distribution at the back of the end-plate) are inaccessible to routine instrumentation. The magnitude of the prying force and the location of its resultant depend on the areas of contact between the connected plates (i.e. column flange and end-plate) and vary with the nature and magnitude of the loading. Because of the complexities of the problem and the considerable number of parameters involved making it impossible to quantify all of them in a design equation, some researchers recommended a simple percentage of the applied flange force in the context of defined proportions of the connection. On the other hand, some researchers have tried to evaluate it accurately,

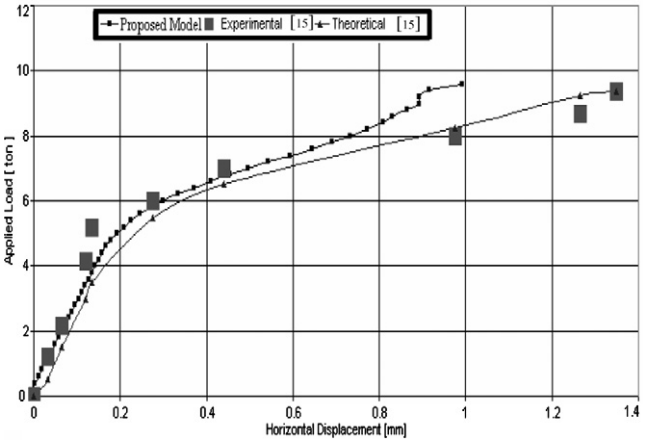

Figure 11 Results at the location of Dial (1).

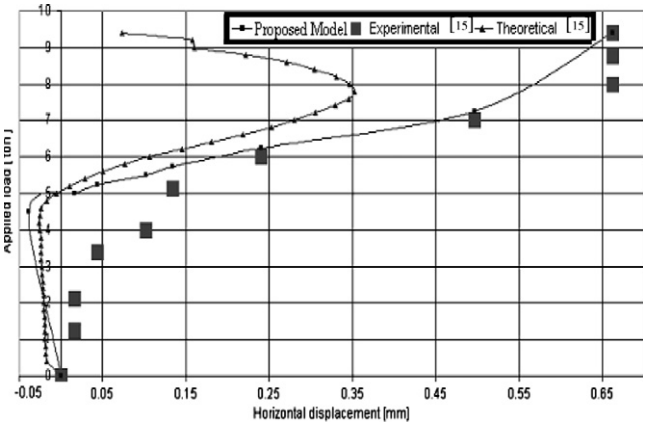

Figure 12 Results at the location of Dial (2).

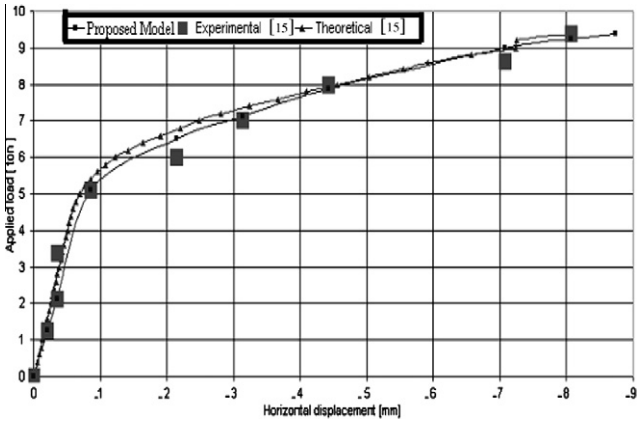

Figure 13 Results at the location of Dial (3).

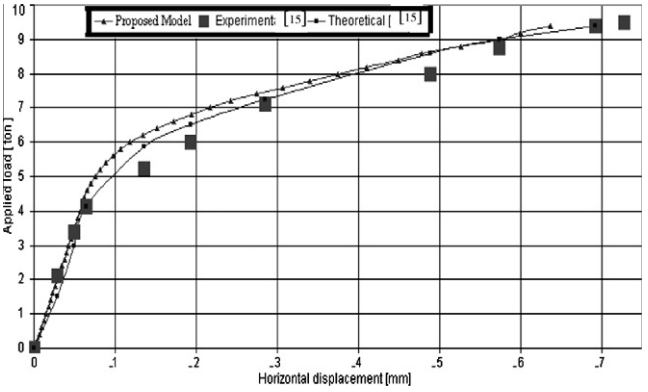

Figure 14 Results at the location of Dial (4).

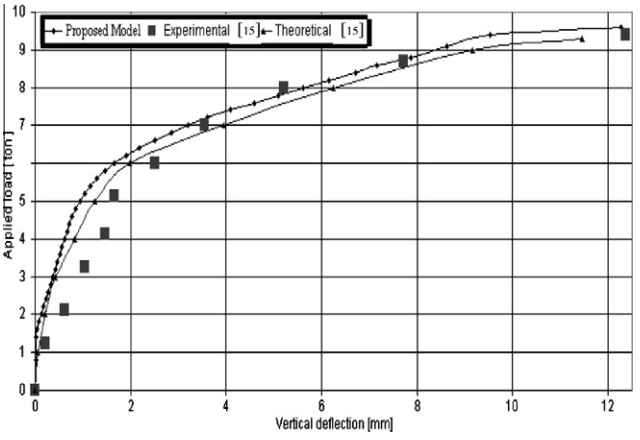

Figure 15 Results at the location of Dial (5).

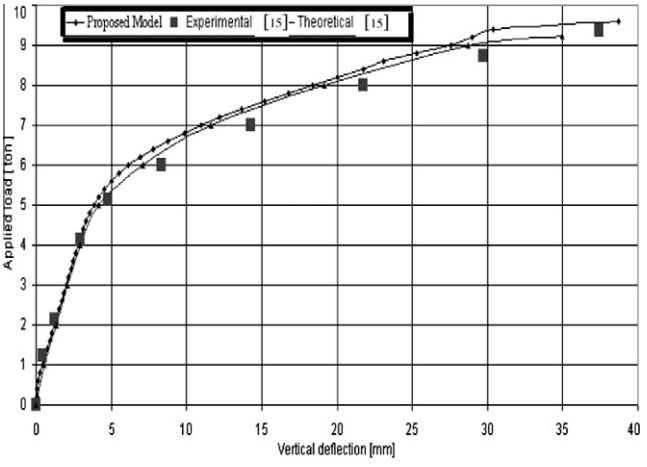

Figure 16 Results at the location of Dial (6).

which led to complicated solutions. Others did not even acknowledge its importance in design.

As shown in Fig. 9, T_1 represents the tension force per bolt transmitted to the extended part of the end-plate and is calculated as ($T_1 = B_1 - C_1$) where B_1 and C_1 are the forces in the outer bolt and its corresponding contact forces, Figs. 7 and 8, respectively. If T_{bf} represents the beam tension flange force carried by two bolts (i.e. one-half of the total flange force), then ($T_2 = T_{bf} - T_1$) where T_2 is the tension transmitted to the bolt beneath the tension flange. For hand-tightened bolts, as mentioned before, $C_1 = Q_1$.

The prying force ratio Q_1/T_1 decreases with increasing the end-plate thickness. The corresponding ratio for the second bolt Q_2/T_2 has the same trend but is smaller in magnitude than Q_1/T_1. Given that the stiffening effect of the beam web is reduced by an increase in end-plate thickness, it tends to equalize the forces T_1 and T_2. Nevertheless, T_1 did not exceed T_2 for the stiffened column connection. (T_1/T_{bf}) increases with increasing end-plate thickness.

2.4.3. Load–deflection relationship

The results of the horizontal displacements in the location of Dials 1–4 and vertical deflections in the locations of Dial 5 and Dial 6, Fig. 1, obtained both experimentally and theoretically by Khalil [15] are compared with those obtained using finite element modeling. Fig. 10 shows the deformed shape

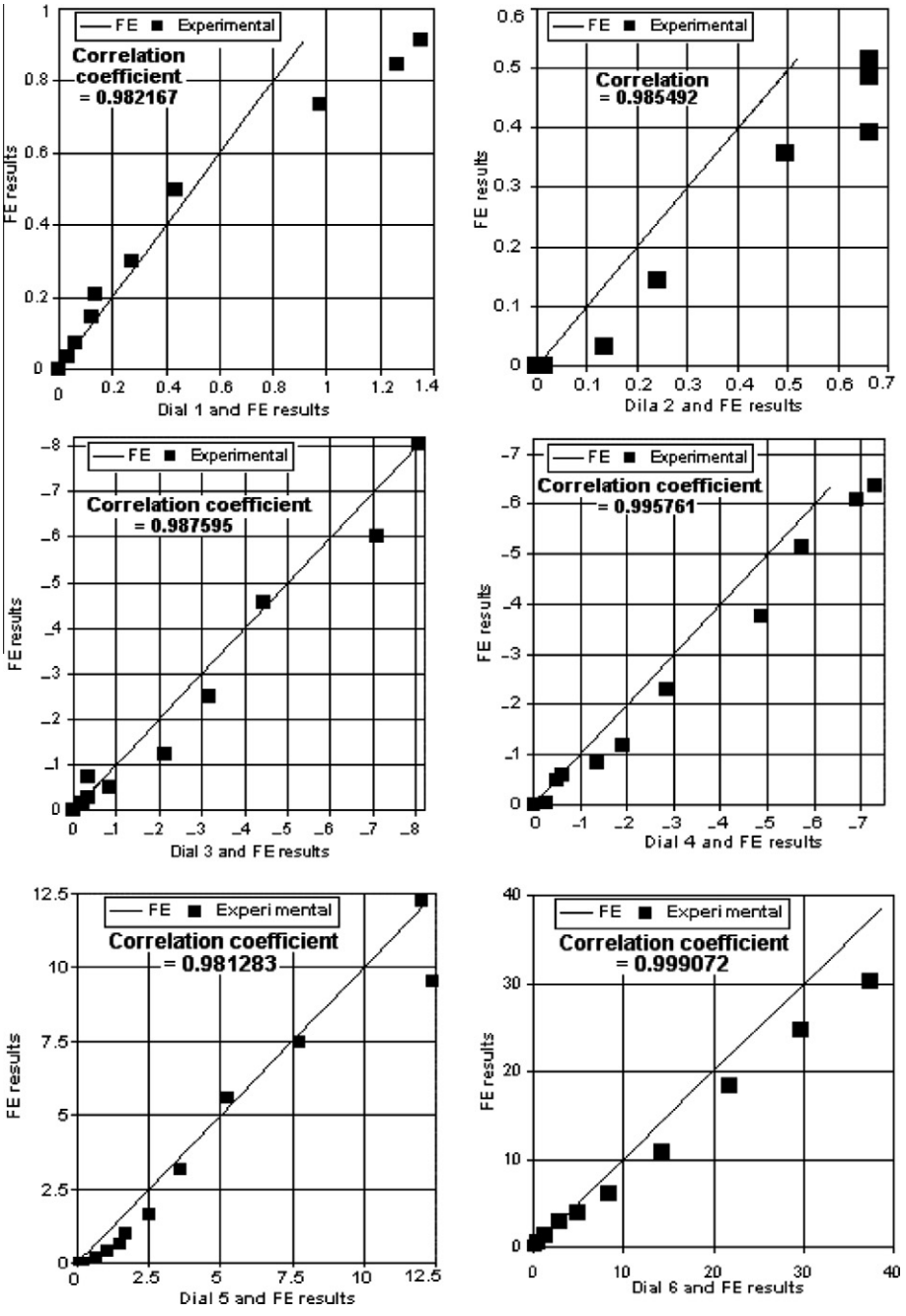

Figure 17 Correlation coefficients between the experimental and FE results for deflections of the tested joint.

of the connection at failure. The most obvious things are the deflection of the beam and the kinking of the panel zone. The results and comparisons of the deflection versus load history are shown in Figs. 11–16. Positive sign means that the horizontal displacement is in the right direction (Z-direction or direction of the beam web) while the positive sign for vertical displacement means downward. The results of the FE model at the location of Dial gauge (2) are different from the experimental results, Fig. 12. Experimentally, Dial gauge (2) is in the region of panel zone kinking and tension bolts which may lead to errors in the very small readings of the dial gauge. Correlation coefficient (Pearson's) is used to find the degrees of association that exists between the experimental deflections [10] and the finite element results. Fig. 17 shows the correlation coefficients for the six dial gauges. Correlation coefficients calculated are 0.982167, 0.985492, 0.987595, 0.995761, 0.981283, and 0.999072 for dials from 1 to 6, respectively, which means a good agreement between both experimental and theoretical (FE) deflections. Failure load in FE model was 9.4 ton while it was 9.38 ton in the experimental model. Figs. 18 and 19 show the total strain and the plastic stresses in the connection at failure, respectively. It is obvious that the panel zone undergoes the majority of strains while bolts are exposed to the maximum plastic stresses in the connection. Generally, the utilized FE model shows very good agreement with both experimental and theoretical results of Ref. [15].

3. Beam-to-column joint under cyclic load

After the unexpected failure of numerous fully-welded beam-to-column connections during the 1994 Northridge California earthquake, a significant amount of the research was made through the SAC Joint Venture [17]. This research was divided

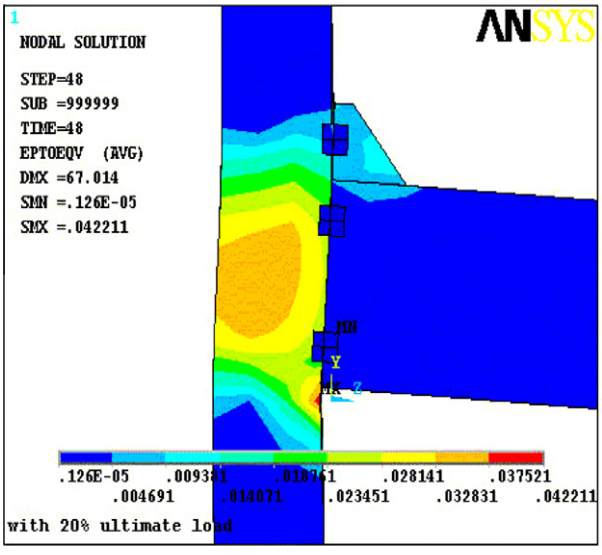

Figure 18 Total strains in the connection.

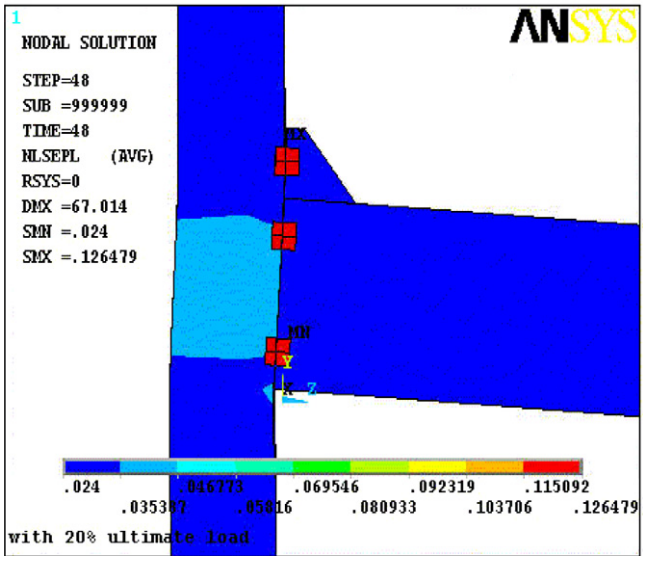

Figure 19 Plastic stresses in the connection.

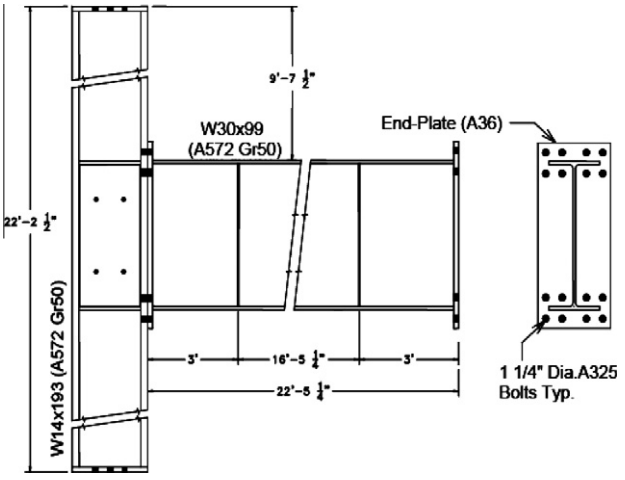

Figure 20 Connection configuration.

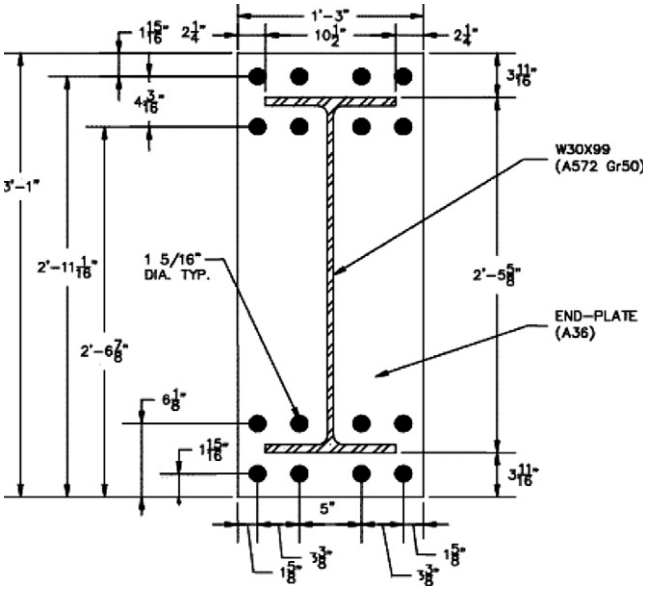

Figure 21 End-plate layout.

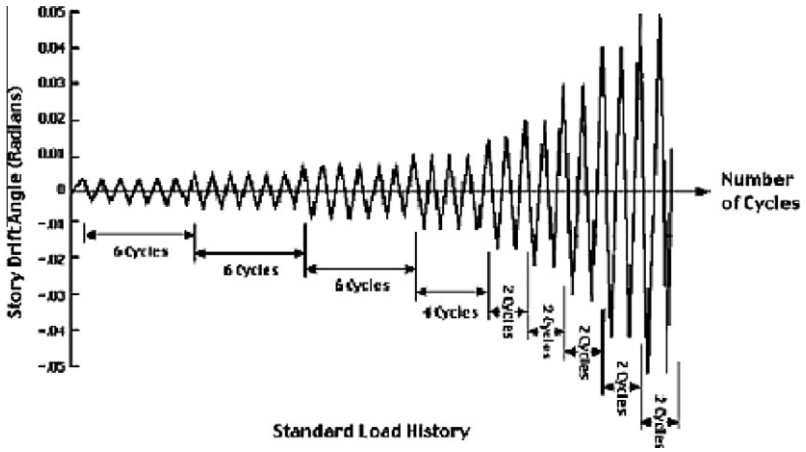

Figure 22 Standard load history recommended by AISC [17].

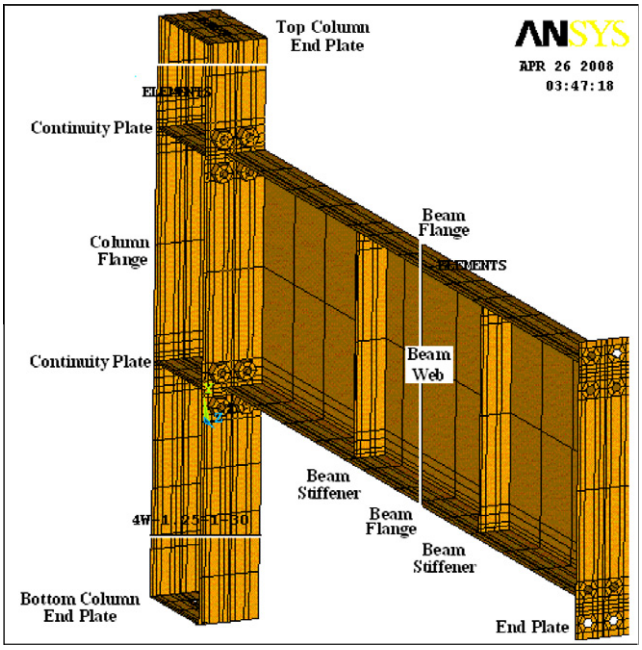

Figure 23 General view of the connection.

into two phases. The initial phase focused on determining the case of the fully-welded connection failures. The second phase focused on finding alternative connections for use in seismic force resisting steel moment frames. The extended end-plate moment connection is one alternative that has been investigated during the second phase of research. The investigation included experimental testing and analytical modeling to determine the suitability of end-plate moment connections for use in seismic force resisting moment frames. A part of these tests was made by Sumner et al. [18–20].

3.1. Joint configuration

The test specimen, chosen to verify the finite element model, consists of a W14x193 (A572 Gr.50) column with a single W30x99 (A572 Gr.50) beam attached to the flange. In this test, the connection was designed to develop 80% of the nominal plastic moment capacity of the beam. The joint configuration and its details are shown in Figs. 20 and 21.

3.2. Loading protocol

The specimen was loaded cyclically according to the standard load history recommended by AISC [21]. In this protocol, the interstory drift angle, θ, imposed on the test specimen is controlled as shown in Fig. 22.

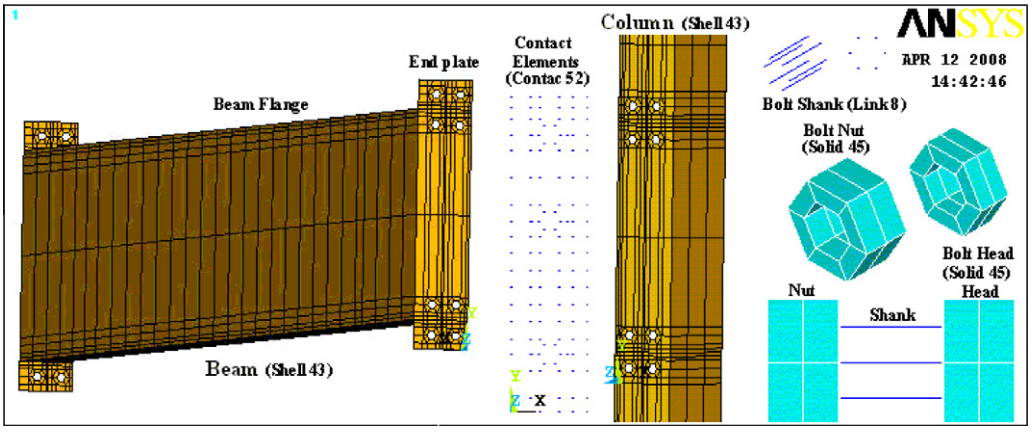

Figure 24 Main components for the modeling of the connection.

3.3. Finite element model

Due to symmetry about a plane passing through the beam and column webs, only one half of the connection is considered in the modeling. Finite element types used in the modeling of beams, columns, end-plates, and bolts are the same as for the previous model. Young's modulus, Poisson's ratio, and Friction coefficient are equal to 29,870 ksi, 0.3, and 0.5, respectively. Figs. 23 and 24 show general view and main components of the analyzed connections, respectively.

Both column ends are hinged supports. Six lateral supports for beam flanges constrained in *X*-direction are provided at a distance of 4 ft. 1 in., 12 ft. 1 in. and 18 ft. 9 in. from the centerline of the column. The free end of the beam is considered as a roller support in the vertical direction. The loading (displacement control) was applied to the centerline of the beam at a node located on the upper flange at a distance of 20 ft. 1 1/4 in. from the centerline of the column.

3.4. Results of the FE model

Table 2 shows a comparison between the experimental results [17] and the FE results.

Figs. 25 and 26 show the relations between the moment at the column centerline and both the total and plastic rotations, respectively; for both experimental and FE models.

Figs. 25 and 26 indicate that there is an increase in softening and stiffening for both loading and unloading stages. This is mainly due to using of node-to-node contact elements CONTAC52. These elements lead to both stiffening and softening according to their being compressed or tensioned, respectively. When the element force is compression, the interface remains in contact and responds as a linear spring leading to increasing of the structure stiffness. As the normal force becomes tension, contact is broken and no force is transmitted leading to decreasing of the structure stiffness. This indicates that element CONTAC52 is not appropriate contact element

Table 2 Results of both models.

Item	Experimental results [17]	FE results	Percentage of error (%)
Maximum applied moment (kips in)	18,521	17,606.425	4.9
Corresponding peak applied load (kips)	76.77	72.98	4.9
Maximum inelastic story drift (rad)	0.021	0.028	33.33
Moment corresponding to the maximum inelastic story drift (kips in)	18,120	17,233.1	4.9

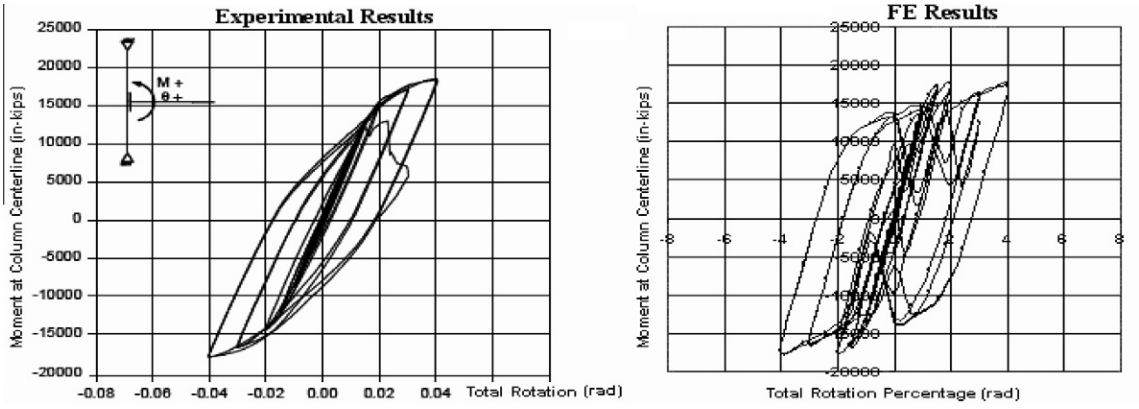

Figure 25 Relation between total rotation and moment at column centerline.

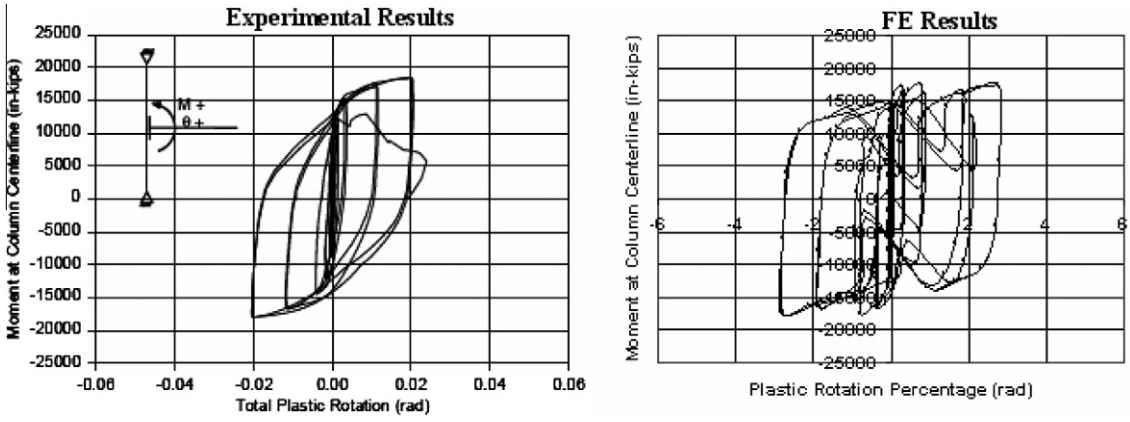

Figure 26 Relation between plastic rotation and moment at column centerline.

for accurate modeling of beam-to-column connection under cyclic loading, although of the high accuracy of the results in Table 2.

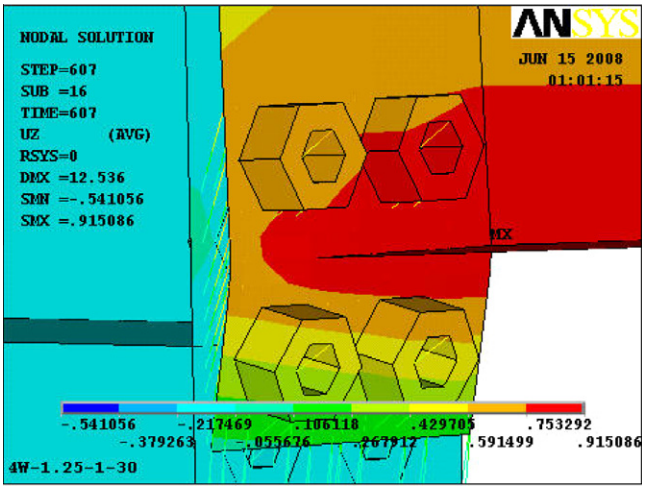

Figure 27 Rupture of the inner two bolts inside the beam bottom flange.

Experimentally, rupture of the two inner bolts inside the bottom flange of the beam and tearing through the thickness of the end-plate between the two inner bolts were observed. In the FE model, rupture in the two inner bolts inside the bottom flange of the beam happened as in the experimental model (Fig. 27). According to the way used in modeling bolts by link elements (shank) between solid elements (head and nut), no clear rupture could be observed. Rupture in the bolt is, instead, realized when the location of the nut is out of the length of the shank, nut is moving away from the end-plate a distance $>(L_{Shank\ Clear} = L_{Shank} - t_{cf} - t_{ep})$ where L_{Shank} is the shank length, t_{cf} the column flange thickness and t_{ep} is the end-plate thickness.

4. Improving of the modeling process

4.1. Defects of the previous modeling

As mentioned before, the details of the FE model used are mainly based on the models presented by Sherbourne and Bahaari [9] and Bahaari and Sherbourne [16]. Although of the high accuracy of the results obtained, there are two main defects:

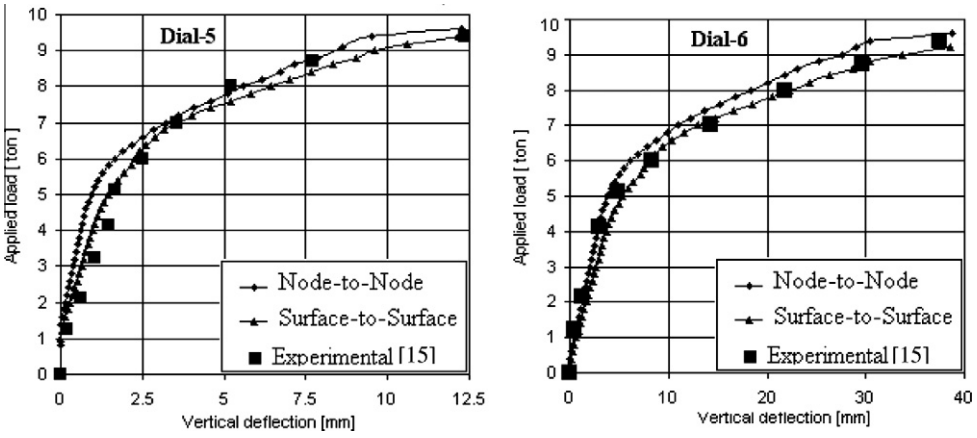

Figure 28 Comparisons of FE models of different contact elements with experimental results.

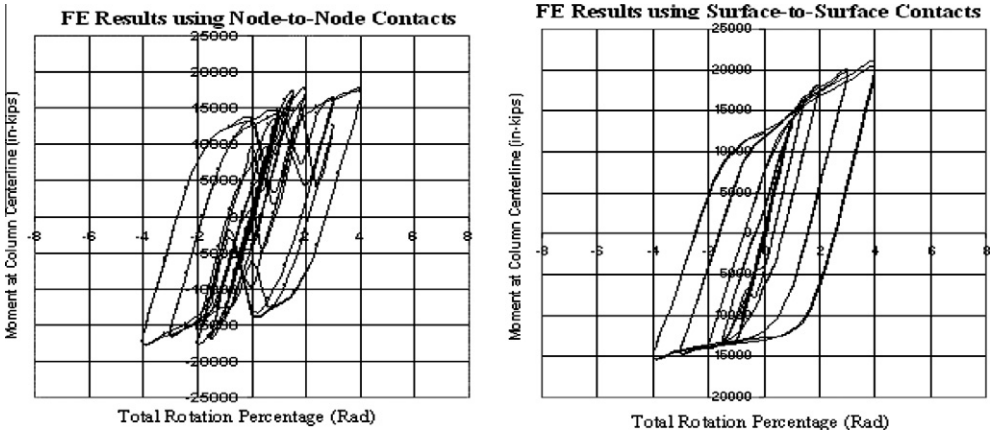

Figure 29 Moment–rotation curve for FE models.

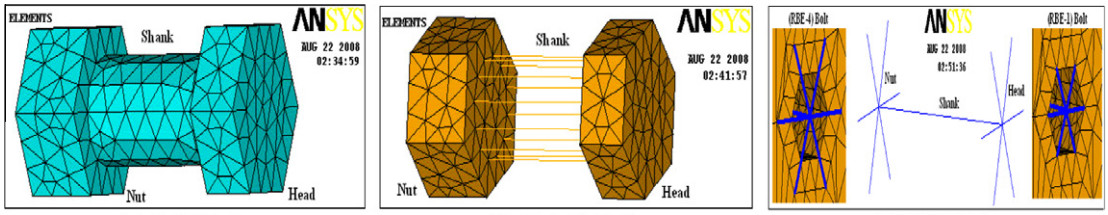

(a) Solid Bolt. (b) Hybrid Bolt. (c) RBE Bolt.

Figure 30 Methods of modeling bolts. (a) Solid bolt; (b) hybrid bolt; (c) RBE bolt.

1. Long time needed for analysis which makes modeling process so expensive and highly time consuming.
2. The inability of contact element CONTAC52 (node-to-node element) to follow the real and usual behavior of moment–rotation curve under cyclic loading.

4.2. Improving the model using surface-to-surface contacts

Finite element model mentioned in Section 2.3 is rebuilt using surface-to-surface contacts (TARGE170 and CONTA173) instead of node-to-node contacts (CONTAC52). Fig. 28 shows comparisons between the results of the experimental model and the two FE models at the location of both Dial 5 and Dial 6. For node-to-node contact model, the correlation values with the experimental results are 0.981283 and 0.999072 for the vertical deflections at the locations of Dial 5 and Dial 6, respectively. These values are, respectively, 0.990011 and 0.997386 for surface-to-surface contact model. Also, using surface-to-surface contact elements decreased the solution time by 60% [15].

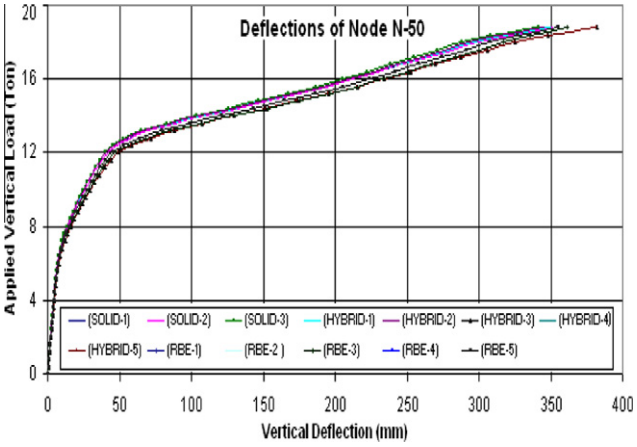

Figure 31 Vertical deflections at node N-50.

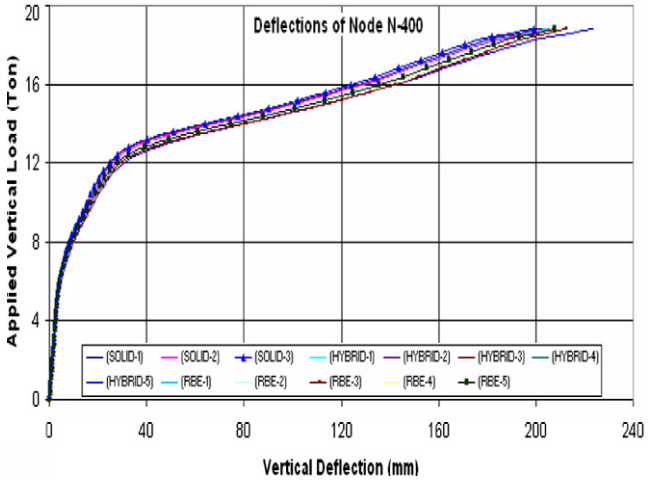

Figure 32 Vertical deflections at node N-400.

Fig. 29 plots moment–rotation curves for the cyclically loaded connection mentioned in Section 3.3 using node-to-node contacts and surface-to-surface contacts. It is obvious that using surface-to-surface contact elements eliminates the defects (subsequent softening and stiffening) that were shown in Figs. 25 and 26.

4.3. Improving the model using other methods for modeling bolts

Modeling of bolts is very critical in finite element modeling of bolted connection as mentioned before. In this section, several methods of modeling bolts in 3D are examined to reach the most suitable and applicable modeling methods taking into account both solution time and accuracy. The joint used previously in Section 3 is used with some modifications in its boundary conditions (both column ends are pinned supports and no axial forces act upon the bottom of the column). A concentrated load is applied at a point 50 mm away from the free beam end. All contact elements used are surface-to-surface contact elements (TARGE170 and CONTA173). Three methods of modeling bolts were chosen namely: solid bolt, hybrid bolt, and rigid body element (RBE) bolt, shown in Fig. 30.

For each model, two nodes along the lower flange of the beam are used to compare results and verifying the methods of modeling bolts. These nodes are 50 mm and 400 mm from the free end of the beam. They are called N-50 and N-400, respectively.

Figs. 31 and 32 show the vertical deflections at nodes N-50 and N-400, respectively, for all the studied models. The curves are so near and cannot be distinguished easily.

5. Proposal for a new technique for modeling bolts

In the previous section, the validity of solid, hybrid, and RBE bolts was verified. However, there is still a need not only to simplify the modeling process but also to save both cost and time. An attempt to do so is conducted by improving a new technique for modeling bolts.

The proposed technique lies between both hybrid bolt and RBE bolt. In this technique, both head and nut are modeled as

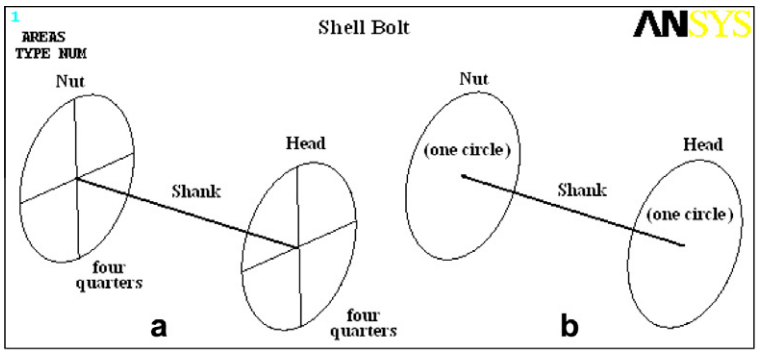

Figure 33 Shell bolt.

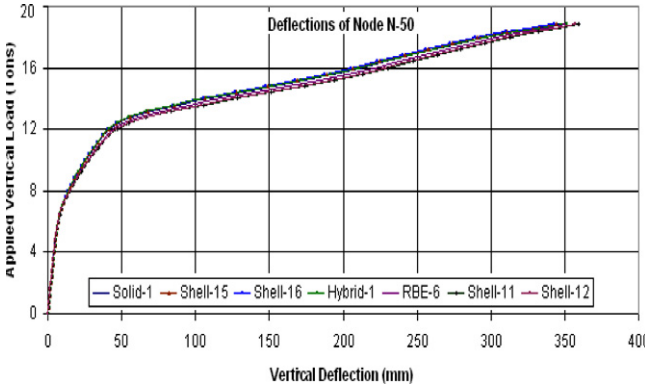

Figure 34 Comparisons between bolts types.

shell elements (shell bolt). This technique is supposed to get rid of the main disadvantage of the RBE bolt which needs extra work for simulating head/nut stiffness as compared to other simulations. Also, it will give much less elements number and hence less solution time than hybrid bolt. The proposed technique for modeling bolts, as shown in Fig. 33, consists of two types of elements:

1. Line elements to model the shank. These elements may be modeled as LINK elements. LINK elements are preferred to be tension only elements to avoid using contact elements at head/nut.
2. Shell elements to model both head and nut. Shell elements may be used in two ways. In the first, SHELL elements cover area equal to the shank area only and the nodes will be coupled. In the second, SHELL elements cover areas equal to the cross-sectional areas of head and nut, respectively.

To examine the proposed bolt modeling and its effect on the solution accuracy, the previous finite element model mentioned in Section 2.3 is used and the examined bolts are modeled as shell bolt with shank modeled as only one line of six LINK10 (tension only) elements. Head/nut areas are equal to the shank area. Nodes are coupled. Both heads and nuts are modeled as four quarters of a circle to easily obtain a node at the center of the circle as shown in Fig. 33A. Head and nut are meshed either mapped or freely. Each one has 12 SHELL43 elements.

Fig. 34 shows the vertical deflections at node N-50 for connections of bolts modeled as shell-bolts comparing with connections of bolts modeled as solid, hybrid and RBE, respectively. The figure shows a very good agreement between these bolt types. This illustrates the advantage of using shell bolts in modeling beam-to-column connections under cyclic loading.

6. Conclusions

1. The FE results and the experimental results are compared to examine the validity and the predictability of the proposed model. The FE results have good agreement with the experimental one at different stages of loading.
2. The FE model can provide a variety of results at any location within the model. A viewing of the full fields of stresses and strains are possible in the FE model. This provides a great advantage in monitoring the components of the connection.
3. Although its of great advantages, it is shown that modeling a beam-to-column connection loaded cyclically is expensive and time consuming in both building and solving the model. So, there is a great need to model the connection more simply and at the same time with an acceptable accuracy.
4. A proposal for a new technique of modeling bolts is presented. The proposal is to model the bolts as a mixing of SHELL elements (for head and nut) and LINK elements (for shank). This technique for modeling of bolts, called SHELL bolt, was examined and compared to other methods for modeling of bolts and was found to be accurate. Also, it needs less time of solution and less storage volume comparing with other techniques for modeling the bolts.

References

[1] American Institute of Steel Construction, Manual of Steel Construction – Load and Resistance Factor Design, first ed., American Institute of Steel Construction, Chicago, 1986.
[2] Eurocode 3, Design of Steel Structures Part 1.1: General Rules and Rules for Buildings, ENV 1993-1-1, Brussels, 1992.
[3] American Institute of Steel Construction, Extended End-Plate Moment Connections, Steel Design Guide S, vol. 4, American Institute of Steel Construction, Chicago, 1990.

[4] Eurocode 3, New Revised Annex J: Joints in Building Frames, ENV 1993-1-1/pr A2, Brussels, 1994.
[5] N. Krishnamurthy, D. Graddy, Correlation between 2 and 3-dimensional finite element analysis of steel bolted end-plate connections, Journal of Computer and Structures 6 (1976) 381–389.
[6] A.R. Kukreti, T.M. Murray, A. Abolmaali, End plate connection moment–rotation relationship, Journal of Constructional Steel Research 8 (1987) 137–157.
[7] A.R. Kukreti, T.M. Murray, M. Ghassemieh, Finite element modeling of large capacity stiffened steel tee-hanger connections, Journal of Computer and Structures 32 (2) (1989) 409–422.
[8] C.P. Chasten, L.W. Lu, G.C. Driscoll, Prying and shear in end plate connection design, Journal of Structural Engineering, ASCE 118 (5) (1992) 1295–1311.
[9] A.N. Sherbourne, M.R. Bahaari, 3D simulation of end-plate bolted connections, Journal of Structural Engineering, ASCE 120 (11) (1994) 3122–3136.
[10] N. Gebbeken, H. Rothert, B. Binder, On the numerical analysis of end plate connections, Journal of Constructional Steel Research 30 (1994) 177–196.
[11] ABAQUS User's Manual, vols. 1 and 2, Version 5.4, Hibbitt, Karlsson and Sorensen, Pawtreket, RI, 1994.
[12] ABAQUS Theory Manual, Version 5.4, Hibbitt, Karlsson and Sorensen, Pawtreket, RI, 1994.
[13] O.S. Bursi, L. Leonelli, A finite element model for the rotational behavior of end plate steel connections, in: Proceedings of the SSRC Annual Technical Session, Chicago, 1994, pp. 163–175.
[14] ANSYS, Release 10.0, Documentation for ANSYS, 2005.
[15] N.N. Khalil, Composite Frames with Semi-Rigid Joints, Ph.D. Thesis, Faculty of Engineering, Tanta University, Tanta, Egypt, 2005.
[16] M.R. Bahaari, A.N. Sherbourne, Structural behavior of end-plate bolted connections to stiffened columns, Journal of Structural Engineering, ASCE 122 (8) (1996) 926–935.
[17] FEMA-355D, 2000i, State of the Art Report on Connection Performance, Prepared by the SAC Joint Venture for the Federal Emergency Management Agency, Washington, DC, 2000.
[18] E.A. Sumner, T.W. Mays, T.M. Murray, End-plate moment connections: test results and finite element method validation, in: Connections in Steel Structures IV: Steel Connections in the New Millennium: Proceedings of the Fourth International Workshop, Roanoke, VA, October 22–25, 2000, pp. 82–93.
[19] E.A. Sumner, T.W. Mays, T.M. Murray, Cyclic Testing of Bolted Moment End-Plate Connections, Research Report SAC/BD-00/21, CE/VPI-ST 00/03, Department of Civil and Environmental Engineering, Virginia Polytechnic Institute and State University, Blacksburg, VA, 2000.
[20] E.A. Sumner III, Unified Design of Extended End-Plate Moment Connections Subject to Cyclic Loading, Ph.D. Thesis, Faculty of the Virginia Polytechnic Institute and State University, Blacksburg, VA, USA, 2003.
[21] American Institute of Steel Construction Inc. (AISC), Manual of Steel Construction – Load and Resistance Factor Design Specification for Structural Steel Buildings, second ed., 1994.